AD-A100 509 MISSION RESEARCH CORP ALBUQUERQUE NM F/G 20/8
COLD-FLUID MODEL OF RESISTIVE INSTABILITIES ON INTENSE RELATIVI--ETC(U)
MAY 81 T P HUGHES, B B GODFREY N60921-80-C-0124
UNCLASSIFIED AMRC-R-285 NL

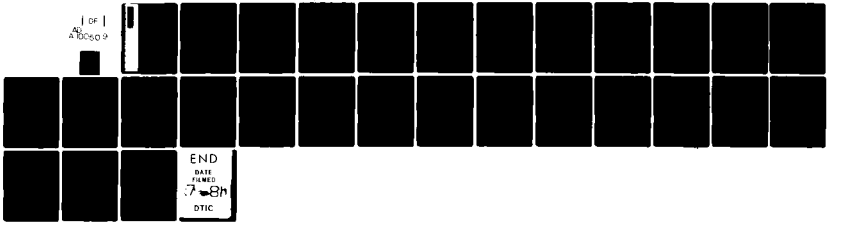

II E

AMRC-R-285

COLD-FLUID MODEL OF RESISTIVE INSTABILITIES ON INTENSE RELATIVISTIC ELECTRON BEAMS

21 May 1981

T. P. Hughes
B. B. Godfrey

Submitted to: Naval Surface Weapons Center
White Oak
Silver Spring, Maryland 20910

Under Contract: N60921-80-C-0124

Submitted by: MISSION RESEARCH CORPORATION
1400 San Mateo Blvd., S. E.
Suite A
Albuquerque, New Mexico 87108

SECURITY CLASSIFICATION OF THIS PAGE (When Data Entered)

REPORT DOCUMENTATION PAGE

READ INSTRUCTIONS BEFORE COMPLETING FORM

1. REPORT NUMBER	2. GOVT ACCESSION NO. AD-A100 509
	3. RECIPIENT'S CATALOG NUMBER
4. TITLE (and Subtitle) COLD-FLUID MODEL OF RESISTIVE INSTABILITIES ON INTENSE RELATIVISTIC ELECTRON BEAMS.	5. TYPE OF REPORT & PERIOD COVERED TECHNICAL REPORT NOVEMBER 1980 - APRIL 1981
	6. PERFORMING ORG. REPORT NUMBER AMRC-R-285
7. AUTHOR(s) T. P. Hughes (MRC) B. B. Godfrey (MRC)	8. CONTRACT OR GRANT NUMBER(s) N60921-80-C-0124
9. PERFORMING ORGANIZATION NAME AND ADDRESS MISSION RESEARCH CORPORATION 1400 San Mateo Blvd., S. E. Suite A ALBUQUERQUE, NEW MEXICO 87108	10. PROGRAM ELEMENT PROJECT, TASK AREA & WORK UNIT NUMBERS 61101E; 0; 0; OR40AA
11. CONTROLLING OFFICE NAME AND ADDRESS Defense Advanced Research Projects Agency 1400 Wilson Blvd., Arlington, VA 22209 Attn: Program Managements/MIS	12. REPORT DATE 21 MAY 1981
	13. NUMBER OF PAGES 26
14. MONITORING AGENCY NAME & ADDRESS(if different from Controlling Office) Naval Surface Weapons Center White Oak, Silver Spring, Maryland 20910 Attn: Code R401	15. SECURITY CLASS. (of this report) UNCLASSIFIED
	15a. DECLASSIFICATION DOWNGRADING SCHEDULE

16. DISTRIBUTION STATEMENT (of this Report)

Approved for public release; distribution unlimited

17. DISTRIBUTION STATEMENT (of the abstract entered in Block 20, if different from Report)

18. SUPPLEMENTARY NOTES

19. KEY WORDS (Continue on reverse side if necessary and identify by block number)

RELATIVISTIC ELECTRON BEAMS
RESISTIVE INSTABILITIES
HOSE INSTABILITY
SAUSAGE INSTABILITY

20. ABSTRACT (Continue on reverse side if necessary and identify by block number)

Resistive instabilities with azimuthal mode numbers m = 0 and 1 are studied on intense, relativistic electron beams. An exact cold-fluid model of the beam is used, and the background is modeled by a scalar conductivity. The effects of the beam profile, the width of the conductivity and return current profiles, and the magnitude of the return current fraction are considered for beams in the 10-100 kA range with γ = 100. Some results for modes with m = 2 and 3 are also presented.

DD FORM 1 JAN 73 1473 EDITION OF 1 NOV 65 IS OBSOLETE

3907

SECURITY CLASSIFICATION OF THIS PAGE (When Data Entered)

CONTENTS

		Page
	ABSTRACT	1
	INTRODUCTION	2
I.	MODELS	3
II.	RESULTS FOR HOSE (m=1) INSTABILITY	6
	A. Step-function current profile: 3 models	6
	B. Effect of nonuniformity in current profile	8
	C. Effect of conductivity and return current profiles	12
III.	RESULTS FOR SAUSAGE (m=0) INSTABILITY	16
IV.	MODES WITH HIGHER m NUMBERS	20
V.	SUMMARY AND CONCLUSIONS	24
	REFERENCES	25

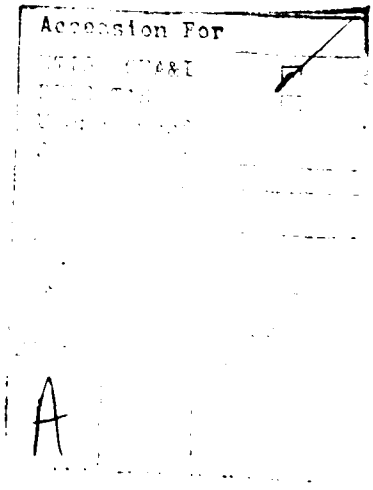

Abstract

Resistive instabilities with azimuthal mode numbers m = 0 and 1 are studied on intense, relativistic electron beams. An exact cold-fluid model of the beam is used, and the background is modeled by a scalar conductivity. The effects of the beam profile, the width of the conductivity and return current profiles, and the magnitude of the return current fraction are considered for beams in the 10-100 kA range with γ = 100. Some results for modes with m = 2 and 3 are also presented.

Introduction

The most serious instabilities of intense electron beams propagating in a highly collisional plasma appear to be the resistive modes[1-3] ($|\omega| \ll 4\pi\sigma$, where ω is the frequency of the mode and σ is the background conductivity). In this report, we pay particular attention to two of these modes, the sausage mode (m = 0, where m is the azimuthal mode number) and hose mode (m = 1). These modes usually have larger growth rates than modes with higher m numbers, and tend to cause gross disruption of the beam. The models we have developed can, however, be used to look at modes with any value of m, and we give some preliminary results for m = 2 and m = 3.

I. MODELS

Our approach is to use the cold-fluid equations to describe the beam. This prevents us from looking at thermal effects and we recognize that present methods of intense beam generation tend to produce beams with a significant thermal spread. We note however that treatments of the resistive hose instability to date [1-4] have emphasized the effect of a spread in betatron frequency (which is present in our cold-fluid model) and that the transverse thermal velocity does not appear explicitly in the dispersion relations. Thus, the importance of a thermal spread as distinct from a spread in betatron frequency is so far unclear. (We are presently developing a model which will be able to address this issue.)

Apart from neglecting thermal effects, our present model makes no additional approximations. It therefore allows us to look at resistive beam modes in a consistent manner, without requiring ad hoc assumptions to take account of radial inhomogeneity. For the most part, we have used the code GRADR[5], modified to include a scalar background conductivity, to solve the complete fluid equations. GRADR computes the linear eigenvalues and eigenfunctions of any self-consistent equilibrium of a cold single-specie beam. In addition, we have made use of analytical dispersion relations obtained from the fluid equations. These dispersion relations apply to beams with square density profiles and are obtained by making the following assumptions, commonly employed in treating resistive instabilities,

$$(\nu/\gamma)^{1/2} \ll 1 \ , \tag{1a}$$

$$|\omega| \ll 4\pi\sigma \ , \tag{1b}$$

$$|\omega a| \ll c \tag{1c}$$

$$|ka| \ll 1 \tag{1d}$$

where ν is the Budker parameter, γ is the beam's relativistic factor, k is the z wavenumber and a is the beam radius. The analytical dispersion relations have the following form, taken from Weinberg[3],

$$\eta \left(\frac{J_m'(qa/\eta)}{J_m(qa/\eta)} \right) + \frac{\xi^2}{qa} = \frac{H_m^{(1)'}(qa) - \alpha_m(qR)J_m'(qa)}{H_m^{(1)}(qa) - \alpha_m(qR)J_m(qa)} \tag{2}$$

where J_m, $H_m^{(1)}$ are Bessel functions of order m, $q = (4\pi i\sigma\omega a^2/c^2)^{1/2}$ with $\mathrm{Im}(q) > 0$, $\alpha_m(qR) = H_{m-1}^{(1)}(qR)/J_{m-1}(qR)$ for $m > 0$, where R is the plasma channel radius, $\alpha_0 = H_1^{(1)}(qR)/J_1(qR)$ and

$$\eta(\lambda) = 1 + \frac{2}{(\lambda-2-m)(\lambda+2-m)}, \tag{3a}$$

$$\xi^2(\lambda) = \frac{4m}{(\lambda-m)(2+m-\lambda)(2-m+\lambda)} \tag{3b}$$

for a single beam specie. In these expressions, $\lambda = \Omega/\omega_\beta \equiv (\omega - kv)/\omega_\beta$ where ω_β is the beam betatron frequency and $v \simeq c$ is the beam z velocity. Two forms of Eq. (2) were employed, one for a single beam specie using Eqs. (3), and one for two counter-rotating species using $\eta_2 = \frac{1}{2}[\eta(\lambda) + \eta(-\lambda)]$, $\xi_2^2 = \frac{1}{2}[\xi^2(\lambda) + \xi^2(-\lambda)]$ in place of η and ξ^2.

We see that the dispersion relation [Eq. (2)] depends only on the dimensionless quantities qa and λ. In what follows, we give our solutions to Eq. (2) and the GRADR dispersion relation in terms of ω/ω_β, kc/ω_β and specify the dimensionless parameter $4\pi\sigma a^2\omega_\beta/c^2$. This is equivalent to obtaining the solutions in terms of qa and λ.

The modified version of GRADR was checked against the single specie dispersion relation [Eqs. (2) and (3)] in the regime where conditions (1) are satisfied. The frequencies obtained agreed to within 1%. GRADR is, of course, not restricted to this regime.

II. RESULTS FOR HOSE (m=1) INSTABILITY

A. Step-function current profile: 3 models.

We compare the dispersion curves obtained from the cold fluid single- and two-species models and the rigid beam model (see, for example, Ref. 4) in Fig. 1, for a regime in which (1a) - (1d) are well satisfied. (The rigid beam dispersion relation is[4]

$$1 = \frac{i\pi}{1-\lambda^2} J_1^2(qa) \left[\frac{H_1^{(1)}(qa)}{J_1(qa)} - \frac{H_0^{(1)}(qR/a)}{J_0(qR/a)} \right] .)$$

All the models agree at low frequency ($|qa| \to 0$), where the dispersion relation becomes

$$k^2 v^2 \simeq -\frac{1}{2} q^2 a^2 (\ell n\, R/a + \tfrac{1}{4}) \omega_\beta^2 \quad , \tag{4}$$

in each case. As one would expect, the graph of γ (the imaginary part of ω) for the single-specie model is not symmetrical about $k = 0$. The dispersion relation for this model has a singularity at $k = k^*$, $\omega = 0$, and this is an accumulation point for an infinity of modes with $k > k^*$ (only the hose mode exists for $0 < k < k^*$). It is not clear what happens to the hose mode at $k = k^*$. However, the curve shown in Fig. 1(b) appears to have the correct continuation of the mode for $k > k^*$.

The single-specie model agrees well with the rigid beam model as to the maximum growth rate. Both disagree with the two-species model by about a factor of 2 (cf. Table I). This is in contrast to recent work[1] which predicts that beam rotation has little effect on the hose mode.

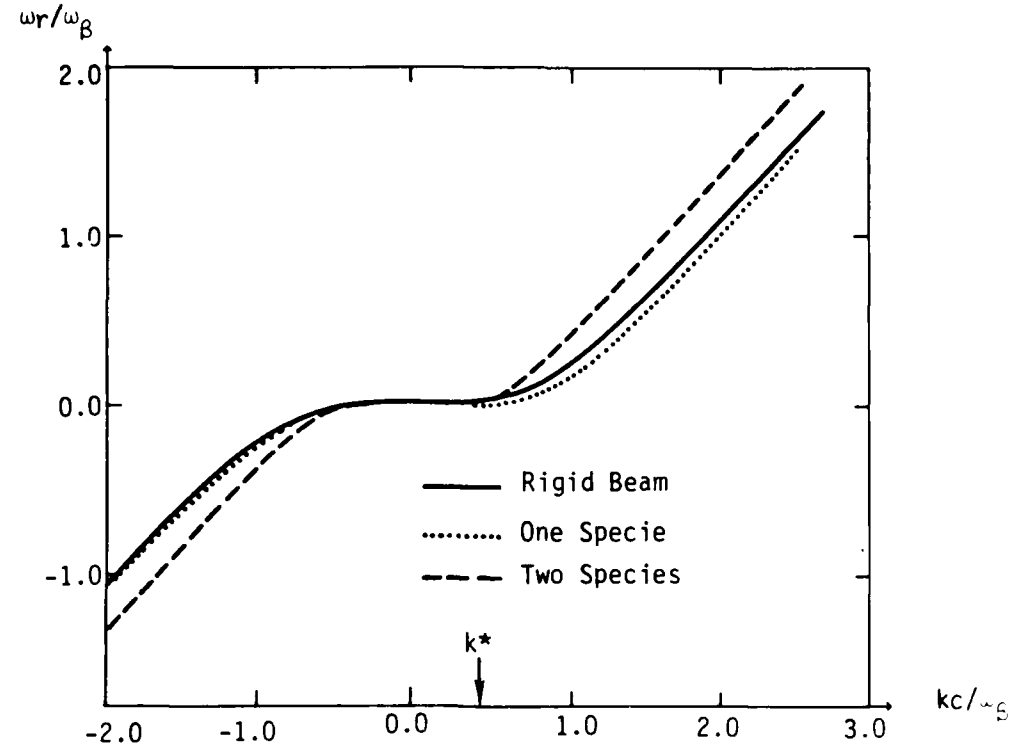

Fig. 1(a)

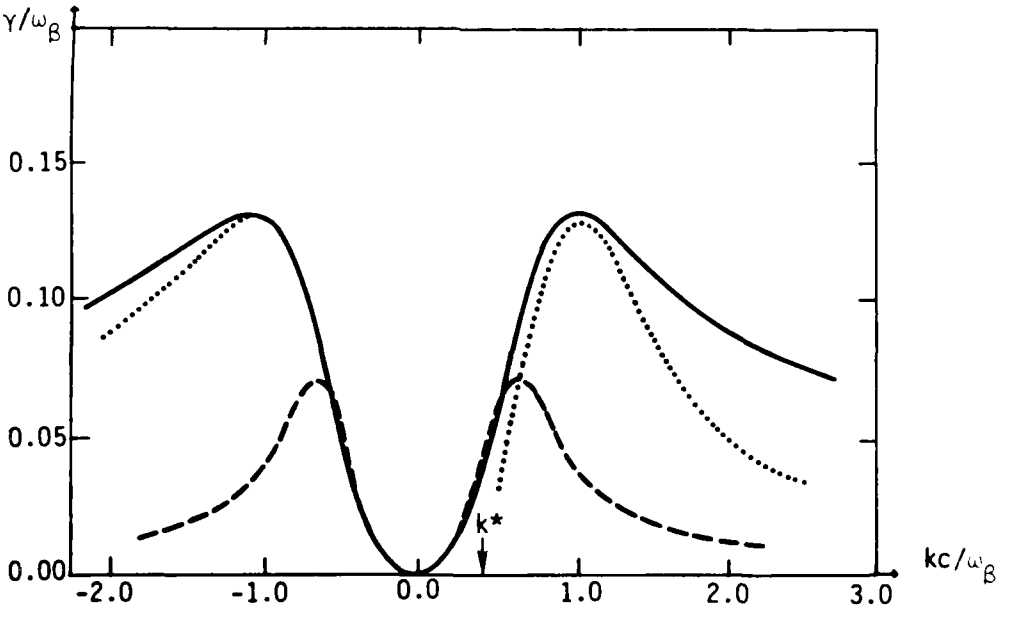

Fig. 1(b)

Figure 1. Comparison between the rigid beam (solid lines), one specie (dotted lines), and two species (dashed lines) models of the hose instability for parameters satisfying (1a) - (1d). The real and imaginary parts of the frequency, ω_r and γ, are plotted versus the z wavenumber, k. There is an accumulation point at k* in the one specie model. We have taken R/a=1 [cf. Eq. (2)].

The difference between the single- and two-species result can, perhaps, be explained by noting that the hose mode is closely associated with the $\omega-kv-\omega_\beta = 0$ (or $\omega-kv+\omega_\beta = 0$) resonance of the beam. For the two-species case, half of the particles are rotating with frequency $-\omega_\beta$ (or $+\omega_\beta$) and respond much less to the perturbing fields than the particles rotating in the opposite direction.

B. Effect of nonuniformity in current profile.

It has been shown[1,2] that the spread in betatron frequency due to nonuniformity in the beam current profile can significantly affect the growth rate and asymptotic behavior of the hose instability. In particular, while the rigid beam model predicts an absolute instability in the beam frame, models with a spread in betatron frequency[1,2] predict that the instability will asymptotically convect backwards along the beam. Our cold-fluid model can, of course, contain a spread in betatron frequency, so that this effect should be present. For nonuniform current profiles, however, we can only obtain ω as a function of k numerically, so that a saddle point analysis of asymptotic behavior would also have to be performed numerically. We have decided to await comparison of the spectra of the present model with those of a more complete model before attempting to do this. For now, we shall concentrate on the maximum growth rate, γ_{max}, obtained from the linear dispersion relation and the corresponding group velocity $v_g(\gamma_{max})$ with which the point of peak amplitude propagates along.

TABLE 1.

Frequency (ω_r, γ) of the most unstable wavenumber k_{max}, for three analytic models.

	Rigid Beam	Single-Species	Two-Species
$k_{max}c/\omega_\beta$	1.0	1.1	.67
ω/ω_β	(0.25, 0.13)	(0.20, 0.13)	(0.11, 0.07)

TABLE II.

Effect of current profile on frequency, phase velocity, v_ϕ, and group velocity, v_g of the most unstable wavenumber. We have chosen $4\pi\bar{\sigma}a^2\bar{\omega}_\beta/c^2 = 16.6$, where $\bar{\sigma}$ is the mean conductivity in the plasma channel and $\bar{\omega}_\beta$ is the r.m.s. betatron frequency; $\bar{\sigma}$, $\bar{\omega}_\beta$ and $\bar{\omega}_\beta a$ are the same for each profile. [$\bar{\omega}_\beta = 6.5\times10^9 sec^{-1}$ for a 10 kA beam with a = 0.5 cm and γ = 100.]

Profile	$k_{max}c/\bar{\omega}_\beta$	$\omega/\bar{\omega}_\beta$	v_ϕ/c	v_g/c
Square	1.25	(0.44, 0.19)	0.35	0.69
Parabolic	1.74	(0.66, 0.26)	0.38	0.72
Gaussian	2.2	(0.64, 0.31)	0.30	0.67
Bennett	3.4	(1.0, 0.44)	0.29	0.72

case with Gaussian beam current and conductivity profiles. We varied the width of the latter, while keeping the peak conductivity, $\sigma(r=0)$, constant. The results in Table III show that the broadening reduces the maximum growth rate. For the broadest profile in this Table the reduction is about 25%, and further broadening has little effect on the growth rate.

So far, we have looked only at cases where the plasma return current is negligible. This is probably a good approximation for beam currents on the order of 10 kA. For beam currents on the order of 100 kA, however, return current fractions, $f \equiv -I_p/I_b$ (I_p = plasma return current, I_b = beam current) near 80% are likely. In looking at the effect of the return current, we have assumed for simplicity that its profile is the same as that of the conductivity profile. In Table IV, we show the effect of changing f, assuming I_p has the same shape as I_b. The presence of a large return current does not have a very dramatic effect on the maximum growth rate. However, the value of k_{max} is rather more sensitive to f. For f = 0, the instability has shifted to larger wavenumbers (cf. Fig. 2) which do not satisfy condition (1d) very well, e.g., $k_{max}r_o$ = 0.36 where r_o is the width of the beam current profile while for f = 0.8, we have $k_{max}r_o$ = 0.13. Condition (1d) is commonly used [1,3] in treatments of resistive modes to justify the neglect of all but the z component of the perturbed beam current density.

The presence of return current causes the beam to be unstable at k = 0 with a purely imaginary frequency, so that the whole beam displaces sideways and may be completely ejected from the plasma channel. This effect is due to the repulsion between the beam and plasma currents.[1]

If the conductivity profile is broadened so that some of the return current flows outside the beam, the maximum growth rate is reduced, as shown in Table V. The largest decrease attained is about 30%. Most of

TABLE III.

Effect of broadened conductivity profiles on hose instability. $\sigma(r=0)$ is the same for each case. As in Table II, we have $4\pi\bar{\sigma}a^2\bar{\omega}_\beta/c^2 = 16.6$.

$\int_0^a \sigma d(r^2)/\int_0^\infty \sigma d(r^2)$	$k_{max}c/\bar{\omega}_\beta$	$\omega/\bar{\omega}_\beta$	v_ϕ/c	v_g/c
1	2.2	(0.64, 0.31)	0.3	0.80
0.9	2.1	(0.54, 0.26)	0.26	0.71
0.8	2.2	(0.60, 0.25)	0.27	0.74
0.6	2.2	(0.58, 0.23)	0.27	0.75

TABLE IV.

Effect of return current fraction f. Return current has same Gaussian profile as beam current, and $4\pi\bar{\sigma}a^2\bar{\omega}_\beta/c^2 = 5.24\times10^2$. [$\bar{\omega}_\beta = 2.1\times10^{10}\text{sec}^{-1}$ for 100 kA beam with a = 0.5 cm and $\gamma = 100.$]

f	$k_{max}c/\bar{\omega}_\beta$	$\omega/\bar{\omega}_\beta$	v_ϕ/c	v_g/c
0.0	2.1	(0.15, 0.10)	0.07	0.64
	k=0.	(0., 0.)	0.	0.
0.8	0.79	(0.15, 0.14)	0.2	0.55
	k=0.	(0., 0.066)	0.	0.

In Table II, we show the effect of increasing the spread in betatron frequency by changing the beam current profile while keeping the total current and average current density constant.

The beam current profiles in each case are, for $0 < r < a$,

Square: $J_b = J_{bo}$,

Parabolic: $J_b = J_{bp}(1 - r^2/a^2)$,

Gaussian: $J_b = J_{bg} \exp(-r^2/r_o^2)$, $r_o = a/2$,

Bennett: $J_b = J_{bb}(1 + r^2/r_b^2)^{-2}$, $r_b = a/3$,

and $J_b = 0$ for $a > a$. The square and Bennett profiles represent extremes in that the former has a single betatron oscillation frequency, while the latter has a uniform spread in $\omega_\beta^2(r)$ from 0 to $\omega_\beta^2(o)$. For these examples the conductivity is assumed to be proportional to the beam density, and the mean conductivity is the same for each profile. The mode considered is the lowest radial eigenmodes, since this is likely to be the one least affected by thermal effects. We see that the maximum growth rate increases, and moves to shorter wavelength, as the profile becomes more peaked on axis. The group velocity changes little.

C. Effect of conductivity and return current profiles.

Ionization produced by secondary electrons (delta rays) is expected to produce significant conductivity outside the beam channel.[6] Furthermore, saturation of the density of ionized electrons within the beam may result in a conductivity profile flatter than that of the beam current. To investigate the effect of broadening the conductivity profile, we chose a

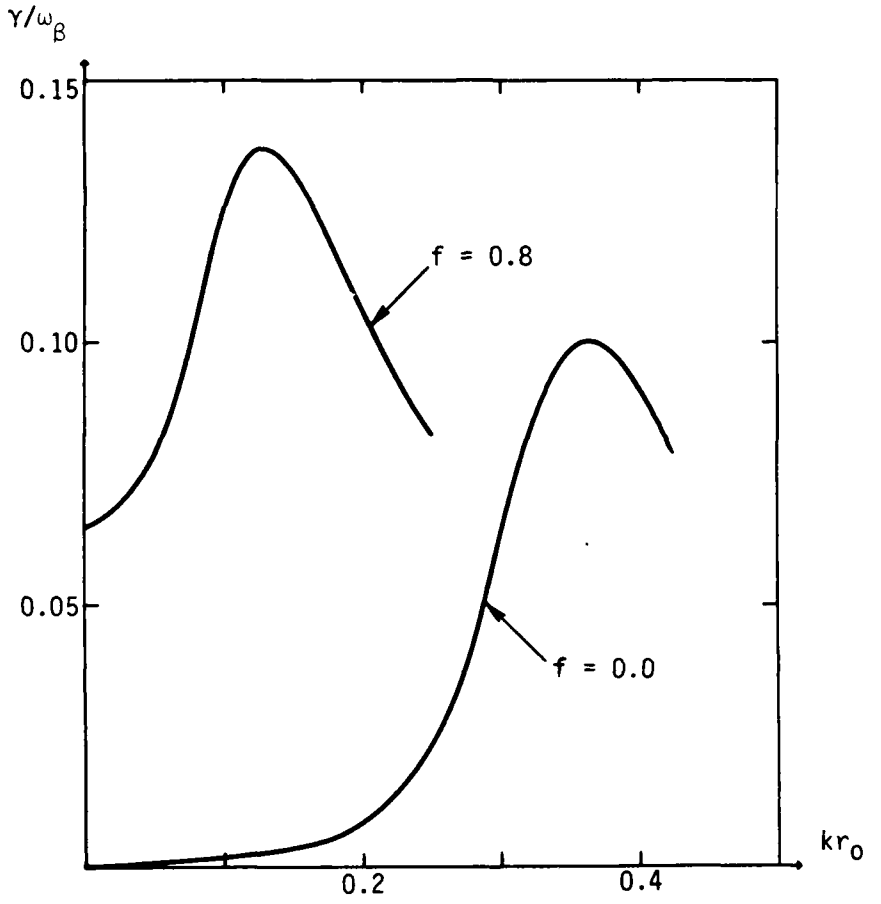

Figure 2. Illustration of the shift in the unstable part of the m = 1 spectrum as a function of the return current fraction f. r_o is the width of the Gaussian beam current profile.

TABLE V.

Effect of broadening the return current profile. In each case, $f = 0.8$. $I_p(a)$ is the return current flowing within the beam. As in Table IV, $4\pi\bar{\sigma}a^2\bar{\omega}_\beta/c^2 = 5.24\times10^2$.

$I_p(a)/I_p$	$k_{max}c/\bar{\omega}_\beta$	$\omega/\bar{\omega}_\beta$	v_ϕ/c	v_g/c
1.0	0.79	(0.15, 0.14)	0.2	0.55
0.9	1.5	(0.18, 0.11)	0.12	0.64
0.8	1.7	(0.18, 0.10)	0.10	0.66
0.6	1.9	(0.18, 0.10)	0.09	0.68
1.0	k=0.	$(0.,6.6\times10^{-2})$	0.	0.
0.9	0.	$(0.,7.4\times10^{-3})$	0.	0.
0.8	0.	$(0.,2.6\times10^{-3})$	0.	0.
0.6	0.	$(0.,1.8\times10^{-3})$	0.	0.

this decrease can be achieved with a small amount of broadening (e.g., 10% of the return current outside the beam). We also see from Table V that broadening leads to a sharp decrease in the growth rate of the k = 0 mode. This is due to the enhanced production of eddy currents outside the beam, which, by Lenz's Law tend to preserve the unperturbed magnetic field configuration.

III. RESULTS FOR SAUSAGE (m = 0) INSTABILITY

In presenting our results for the sausage instability, we shall again consider only the lowest radial eigenmode. We have looked at the next higher mode and found it to be roughly 50% more unstable than the fundamental. However, the higher mode should be more affected by thermal effects, and until we have had an opportunity to consider these effects, we shall postpone presentation of the cold-fluid results for this higher mode.

As in the case of the hose instability, we shall consider beams in the 10 kA (f = 0) and 100 kA (f ≈ 0.8) regimes, and examine the effect of varying f and of broadening the conductivity and return current profiles. Gaussian profiles are used throughout. The results are summarized in Tables VI, VII and VIII. From Table VI, we see that broadening the conductivity profile reduces the m = 0 growth rate by no more than 7% (cf. 25% reduction for m = 1). Conversely, the presence of a large return current fraction has a smaller destabilizing effect than for m = 1, as can be seen by comparing Table VII with Table IV.

For the case of a beam with f = 0.8, broadening the return current and conductivity profiles leads to a reduction of about 10% in maximum growth rate, as can be seen from Table VIII. Note that this is consistent with the results in Tables VI and VII, namely, (1) the weak effect of broadening σ and (2) a 10% decrease in γ_{max} as f goes from 0.8 to 0.

As we decrease f, k_{max} increases [roughly as $(1-f)^{1/2}$], just as we found in the case of the m = 1 instability (cf. Fig. 3). In the present instance, we have $k_{max}r_0 = 0.28$ for f = 0.8, and $k_{max}r_0 = 0.69$ for f = 0. Again, this tends to violate condition (1d), which may explain the discrepancy between our results and those of Lee,[7] who finds that for f = 0, beams with Gaussian profiles are stable.

TABLE VI.

Effect of broadened conductivity profiles on the sausage instability for $4\pi\bar{\sigma}a^2\bar{\omega}_\beta/c^2 = 16.6$ [cf. Table III].

$\int_0^a \sigma d(r^2)/\int_0^\infty \sigma d(r^2)$	$k_{max}c/\bar{\omega}_\beta$	$\omega/\bar{\omega}_\beta$	v_ϕ/c	v_g/c
1.0	4.7	(1.4,0.33)	0.3	0.82
0.9	5.0	(1.6,0.31)	0.3	0.86
0.8	5.0	(1.6.0.31)	0.3	0.86
0.6	5.0	(1.6,0.31)	0.3	0.86

TABLE VII.

Effect of the magnitude of the return current fraction f on the sausage instability. I_b, I_p, and σ all have the same profile, and $4\pi\bar{\sigma}a^2\bar{\omega}_\beta/c^2 \approx 5.24\times10^2$ [cf. Table IV].

f	$k_{max}c/\bar{\omega}_\beta$	$\omega/\bar{\omega}_\beta$	v_ϕ/c	v_g/c
0.8	1.6	(0.29, 0.17)	0.18	0.66
0.64	2.3	(0.29, 0.16)	0.13	0.68
0.25	3.4	(0.29, 0.15)	0.08	0.69
0.0	4.0	(0.29, 0.15)	0.07	0.7
0.8	k=0.	(0., 0.03)	0.0	0.0
0.64	0.	(0., 6.3×10^{-3})	0.0	0.0
0.0	0.	(0., 0.)	0.0	0.0

TABLE VIII.

Effect of broadening the return current profile (along with the conductivity profile); f = 0.8 and $4\pi\bar{\sigma}a^2\bar{\omega}_\beta/c^2 = 5.24\times10^2$ throughout. [cf. Table V].

$I_p(a)/I_p$	$k_{max}c/\bar{\omega}_\beta$	$\omega/\bar{\omega}_\beta$	v_ϕ/c	v_g/c
1.0	1.6	(0.29, 0.17)	0.18	0.66
0.9	3.0	(0.34, 0.17)	0.11	0.65
0.8	3.3	(0.34, 0.16)	0.10	0.7
0.6	3.6	(0.31, 0.15)	0.09	0.7
1.0	$k=0.$	(0., 0.03)	0.	0.
0.9	0.	$\simeq$ 0.	0.	0.

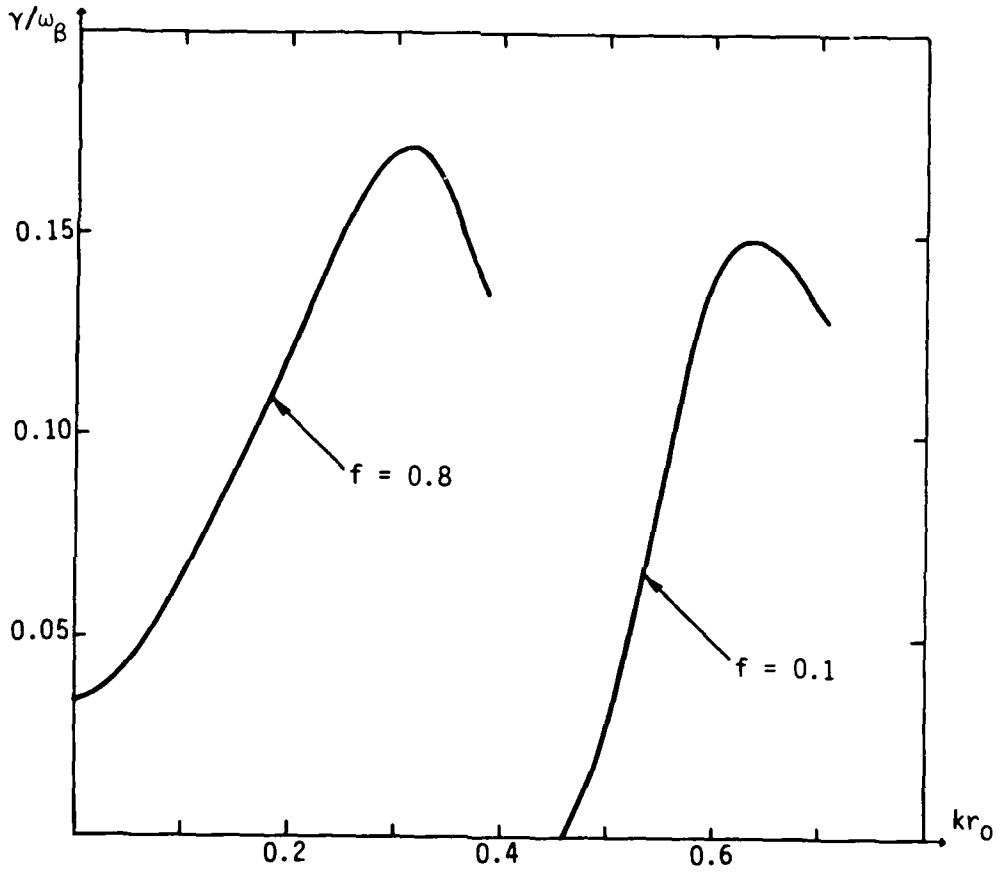

Figure 3. Illustration of the shift in the unstable part of the m = 0 spectrum as a function of f.

As in the case of the hose mode, the beam has an unstable sausage mode at $k = 0$ for $f \neq 0$, whose growth rate increases with f (see Table VII). However, the growth rate is significantly smaller than that of the $k = 0$ hose mode (cf. Table IV), and is drastically reduced for broadened conductivity and return current profiles (see Table VIII).

IV. MODES WITH HIGHER m NUMBERS

To date, modes with $m > 1$ have received little attention in the context of self-pinched electron beams. It is thought that these may be strongly damped by the spread in betatron frequency of a radially inhomogeneous beam. We have not looked in detail at $m > 1$ modes with our present model since the higher the m number, the more important thermal effects are likely to be. However, we have obtained some preliminary results for the $m = 2, 3$ modes using the two-species version of Eq. (2). The results are presented in Table IX and Fig. 4 along with results for $m = 0, 1$ from the same dispersion relation. We have used Weinberg's notation[3] to denote the modes, dividing them into four groups, A_{mn} B_{mn}, C_m and D_m. Thus, for example, A_{mn} denotes a mode with azimuthal number m and radial mode number n (n radial zeroes). In this notation, A_{01} denotes the fundamental sausage mode and C_1 denotes the hose mode. For a given value of m, the A and B series (when they exist) have an infinite number of members, which at low frequencies come together at accumulation points (cf. Fig. 4). We have only looked at the first two members in each case. We see that all the modes for $m = 0$-3 have comparable maximum growth rates. Also, the higher frequency modes (B, D) have $v_g/c \simeq 1$ so that the point of maximum growth rate convects at near the beam velocity. We feel that these results call for a closer look to be taken at the higher m number modes using a more complete model for the beam.

TABLE IX.

Comparison of modes with m = 0 to 3 for square-profile, cold, non-rotating beam. In general, there are four sets of modes for each m, A_{mn} ($n=1 - \infty$), B_{mn}, C_m, D_m, although some of these are missing at low m-values. We have $4\pi\bar{\sigma}a^2\bar{\omega}_\beta/c^2 = 16.6$ throughout.

Mode	$k_{max}c/\bar{\omega}_\beta$	$\omega/\bar{\omega}_\beta$	v_ϕ/c	v_g/c
A_{01}	2.7	(1., 0.20)	0.35	0.85
A_{02}	4.5	(2.7, 0.27)	0.61	0.90
A_{11}	1.2	(0.4, 0.15)	0.33	0.72
A_{12}	2.2	(1.4, 0.17)	0.63	0.90
B_{11}	4.9	(2.0, 0.10)	0.41	0.95
B_{12}	6.4	(3.5, 0.11)	0.55	0.95
C_1	0.66	(0.17, 0.11)	0.26	0.61
B_{21}	6.7	(2.8, 0.10)	0.42	1.0
B_{22}	7.5	(3.6, 0.10)	0.49	1.0
D_2	3.0	(1.2, 0.08)	0.39	0.95
A_{31}	0.58	(1.7, 0.12)	2.9	0.95
A_{32}	3.2	(4.3, 0.12)	1.35	0.95
B_{31}	$\simeq$ 8.0	$\simeq$ (3.2, 0.10)	0.4	0.95
B_{32}	$\simeq$ 8.0	$\simeq$ (3.2, 0.10)	0.36	1.0
C_3	difficult to track; appears to join onto an A mode.			
D_3	5.1	(2.3, 0.08)	0.45	0.98

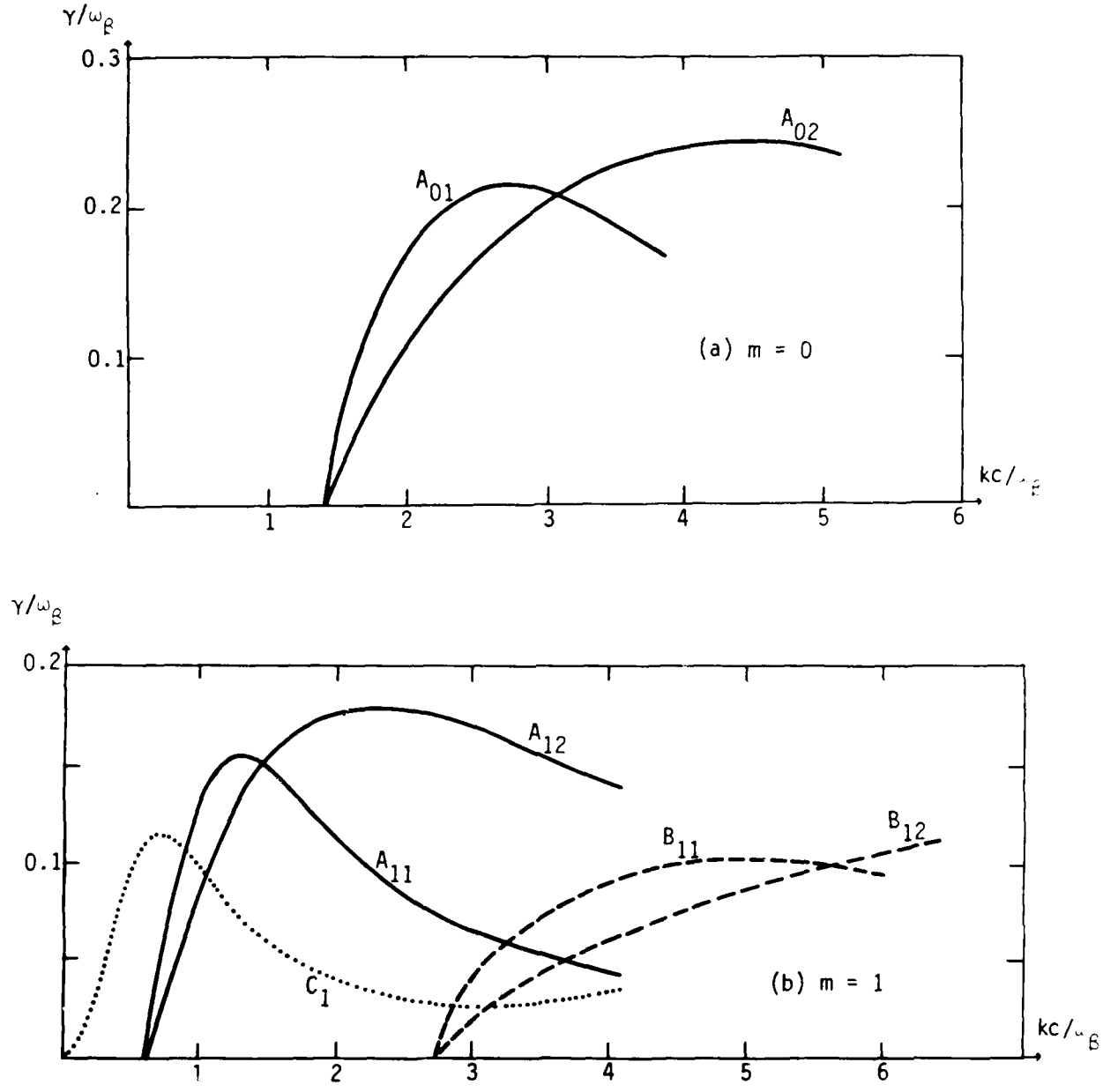

Figure 4. Comparison of the growth rates of resistive modes with m = 0 to m = 3. The two-species version of Eq. (2) is used here. Only the first two members of the A and B series are shown. We have taken R/a=1.

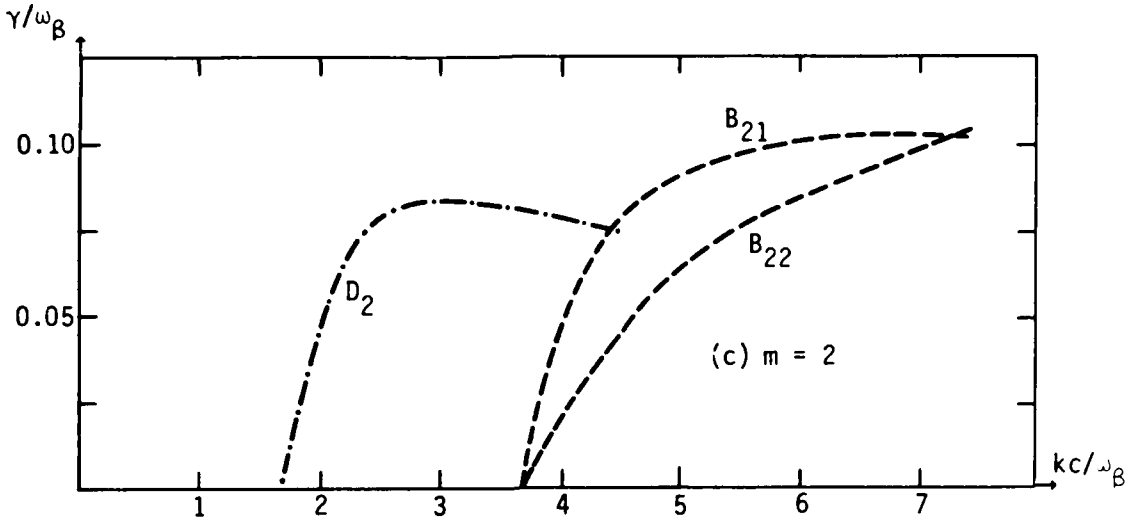

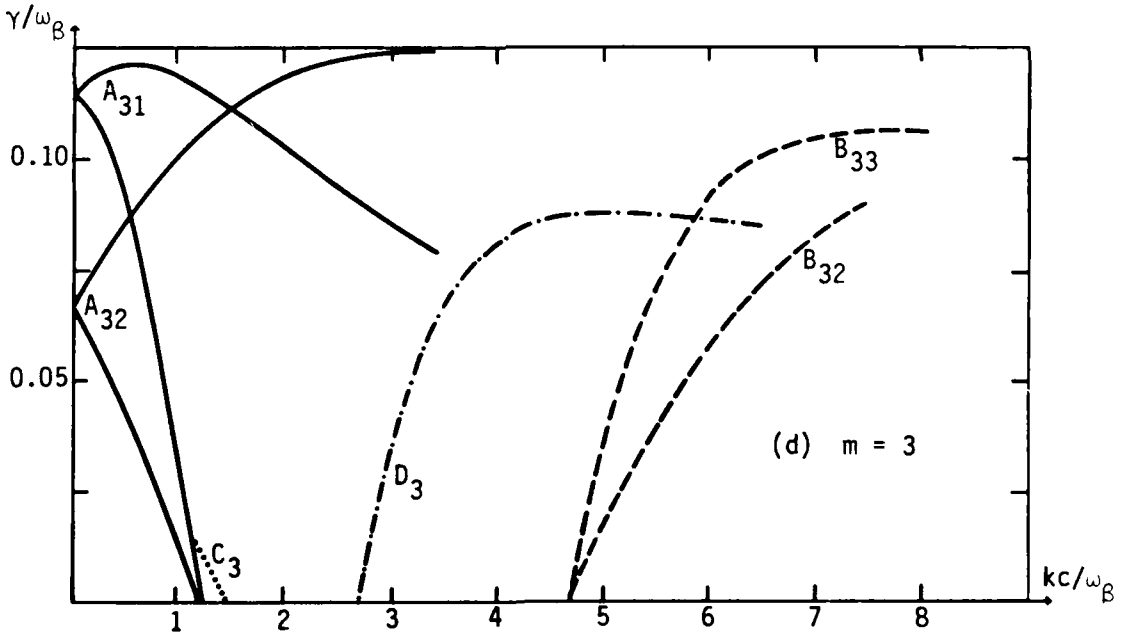

Figure 4. Continued.

V. SUMMARY AND CONCLUSIONS

We have studied the growth rates and group velocities of the m = 0 and m = 1 resistive beam instabilities using an exact cold-fluid model for the beam and a scalar background conductivity. In particular, we have looked at the effects of the beam current profile, the width of the conductivity and return current profiles, and the magnitude of the return current fraction, f. For the most part, we used Gaussian profiles for the beam and return currents and for the conductivity, and we considered beams in the 10 kA (f = 0) and 100 kA (f $\simeq$ 0.8), regimes with γ = 100. We find that broadening the conductivity and return current profiles leads to some reduction in maximum growth rates ($\lesssim$ 10% for m = 0, $\lesssim$ 30% for m = 1). The main effect of reducing f is to shift the instabilities to shorter wavelengths. We note some discrepancies between our results and those of other workers, e.g., the dependence of m = 1 growth rates on beam rotation, and the stability of radially nonuniform beams to the m = 0 mode. Finally, we have presented some preliminary results on modes with m = 2, 3 which show that for a square beam profile, the growth rates are comparable to those for m = 0 and 1. Work is in progress on a more complete model with which we hope to resolve the discrepancies mentioned, and also obtain more accurate results in general than is possible with the present model.

REFERENCES

1. H. S. Uhm and M. Lampe, Phys. Fluids 23, 1574 (1980); H. S. Uhm and M. Lampe, NRL Memorandum Report No. 4441 (1981).

2. E. P. Lee, Phys. Fluids 21, 1327 (1978); E. J. Lauer, R. J. Briggs, T. J. Fessenden, R. E. Hester, and E. P. Lee, ibid., p. 1344.

3. S. Weinberg, J. Math. Phys. 8, 614 (1967).

4. E. P. Lee, Lawrence Livermore National Laboratory, UCID-16268 (1973).

5. B. B. Godfrey, Mission Research Corporation, AMRC-R-223 (1980).

6. N. Carron, private communication.

7. E. P. Lee, Lawrence Livermore National Laboratory, UCID-18940 (1981).

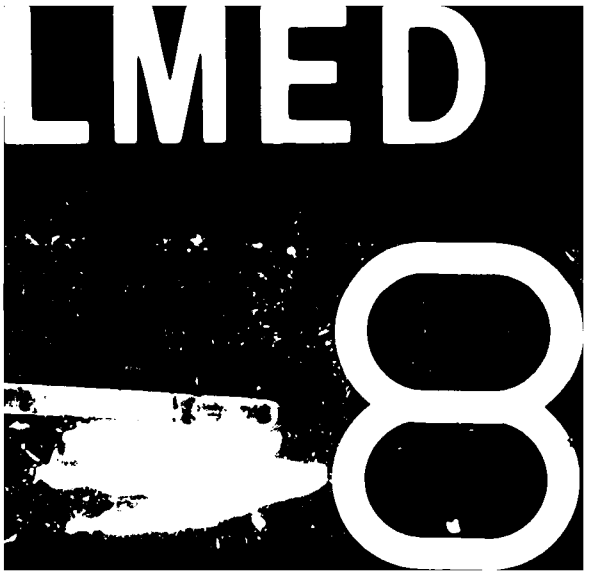
LMED
8